Supporting Information

Polymorphous supercapacitors constructed from flexible three-dimensional carbon network/polyaniline/MnO_2 composite textiles

Jinjie Wang,[†] Liubing Dong,[*,†,‡] Chengjun Xu,[*,†] Danyang Ren,[†,‡] Xinpei Ma,[†,‡] Feiyu Kang [†,‡]

[†] Graduate School at Shenzhen, Tsinghua University, Shenzhen 518055, China

[‡] School of Materials Science and Engineering, Tsinghua University, Beijing 100084, China

[*]Corresponding authors:

L. Dong (dong1060@126.com); C. Xu (vivaxuchengjun@163.com)

Experimental section

1. Calculation method

Calculation method for capacitance, energy density and power density of different electrodes/supercapacitors was according to **References S1-S2**.

2. Configuration of asymmetric textile supercapacitors

To construct asymmetric textile supercapacitors, APCM textile was chosen as positive electrode and ACFC thick electrode composed of two layers of ACFC textile as negative electrode. The ACFC thick electrode shows large areal capacitance of 4599 mF cm^{-2} at the current density of 10 mA cm^{-2} (this will be discussed in following content). In order to optimize the performance of the asymmetric textile supercapacitors, charge of the positive electrode and negative electrode should be balanced according to the equation $Q = C \times \Delta V \times A$, where "C" is specific capacitance of the electrode, "ΔV" is the potential window and "A" is the area of the electrode.[S3] To achieve $q_+ = q_-$, the areal balance of electrodes was calculated by the equation $\frac{A_+}{A_-} = \frac{C_- \times \Delta E_-}{C_+ \times \Delta E_+}$. Therefore, the area ratio between positive electrode and negative electrode was calculated to be 0.998.

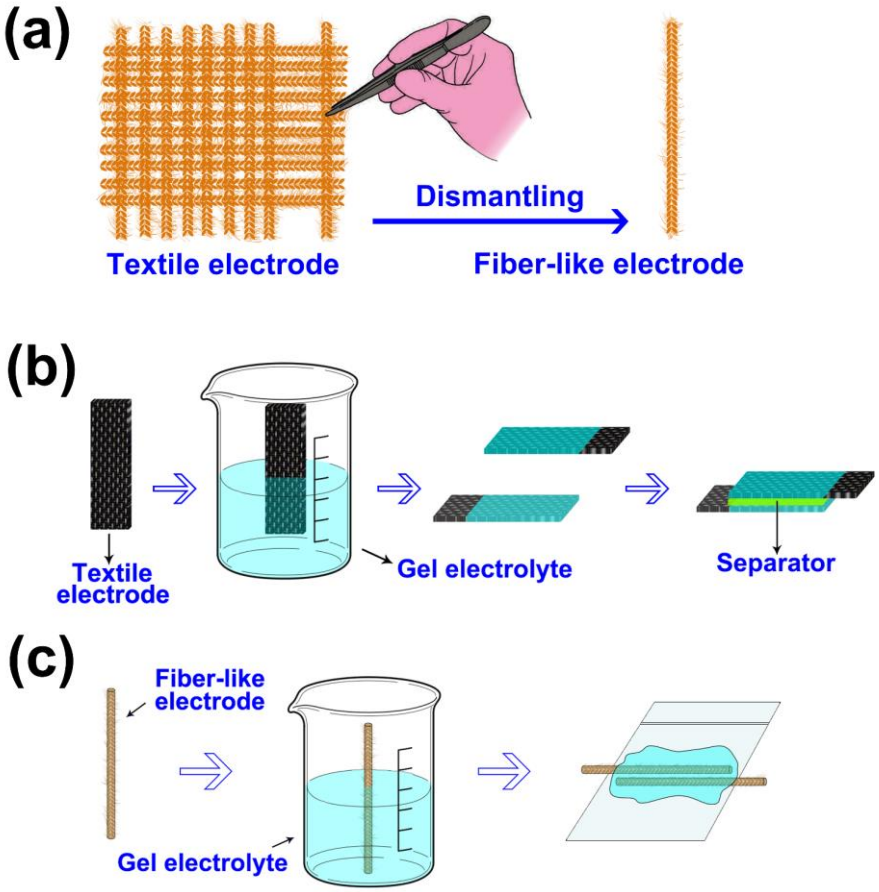

Figure S1. Fabrication schematics of (a) fiber-like electrode, (b) solid-state flexible textile supercapacitor and (c) solid-state flexible fiber-like supercapacitor.

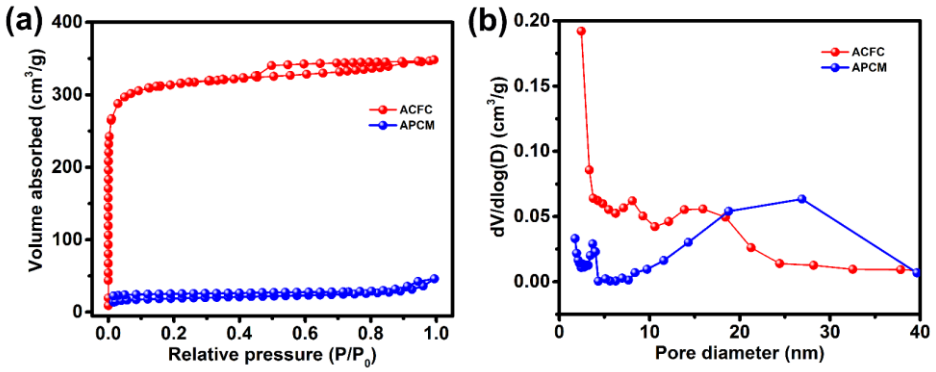

Figure S2. (a) Nitrogen adsorption-desorption isotherms and (b) pore size distribution curves of ACFC and APCM textiles. The specific surface area of ACFC and APCM are 1242 m^2 g^{-1} and 62 m^2 g^{-1}, respectively. Significant decrease of BET surface area of the textile after deposition of PANI-CNT-MnO_2 is caused by the following reasons: (1) PANI, CNTs and MnO_2 coat on fiber surface, leading to the "disappearance" of some pores originally exist on carbon fibers; (2) specific surface area of CNTs is only 150~210 m^2 g^{-1}, much lower than that of pure ACFC.[S1-S2]

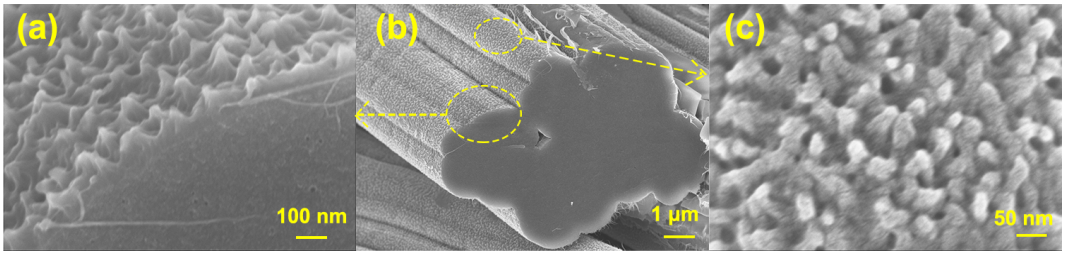

Figure S3. (a)-(c) Morphologies of PANI on activated carbon fiber surface in AP textile.

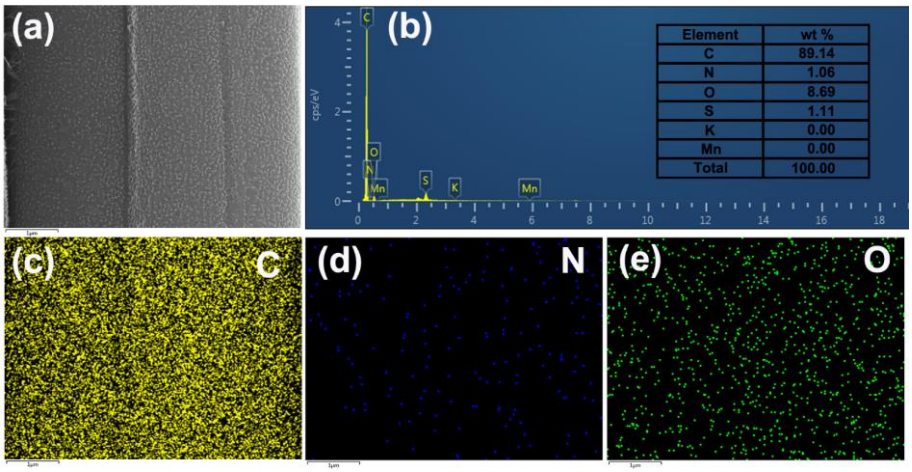

Figure S4. (a) SEM image and (b)-(e) EDS mapping of carbon fiber surface in AP textile.

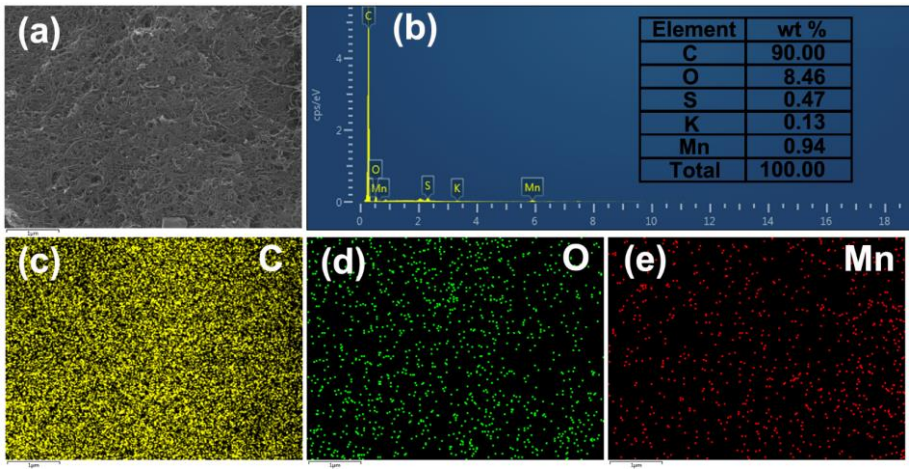

Figure S5. (a) SEM image and (b)-(e) EDS mapping of carbon fiber surface in APCM textile.

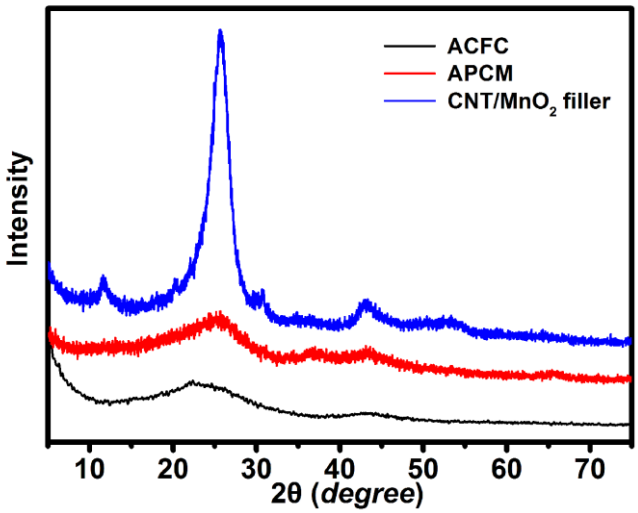

Figure S6. XRD patterns of ACFC, APCM and MnO_2/CNT fillers. The XRD pattern indicates a type of birnessite MnO_2 (JCPDS#42-1317).

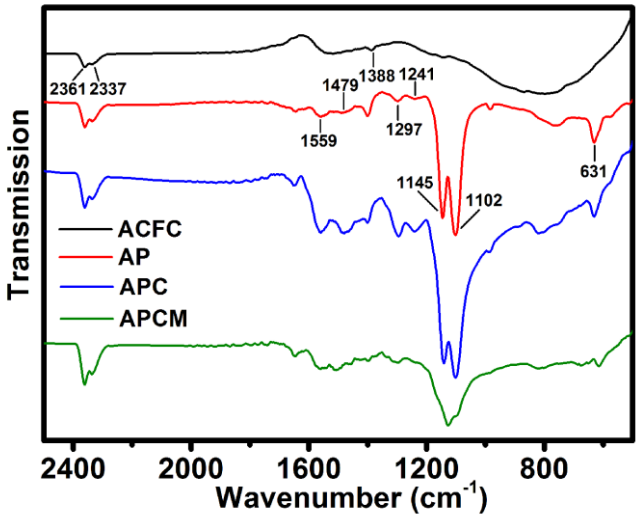

Figure S7. FTIR spectra of different textile electrodes. In the FTIR spectrum of ACFC, the peaks around 1388 and 2337~2361 cm^{-1} are attributed to the COO- functional group and absorption of CO_2. In the FTIR spectrum of AP, the band at 631 cm^{-1} corresponds to the absorption of SO_4^{2-}. The FTIR spectra of APC and APCM are similar to the spectrum of AP. The spectra of the composite textiles exhibit clearer bands at 1200~1600 cm^{-1} which is attributed to the better interaction between CNT and PANI.[S4]

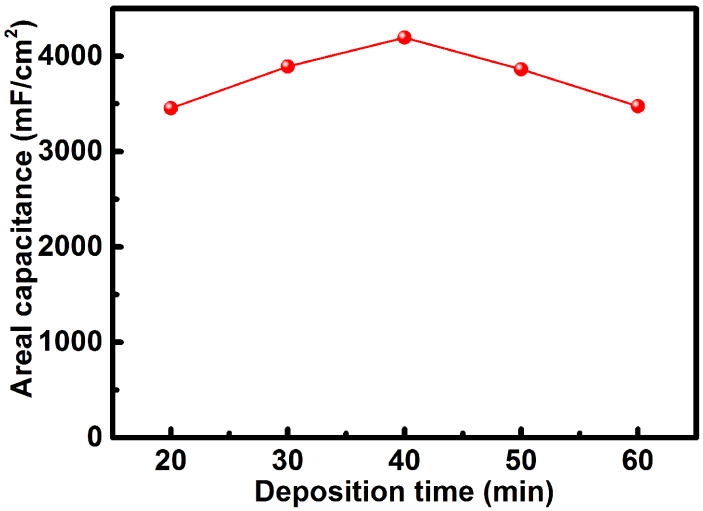

Figure S8. Areal capacitance of the ACFC/PANI composite textile electrodes prepared with different deposition time of PANI.

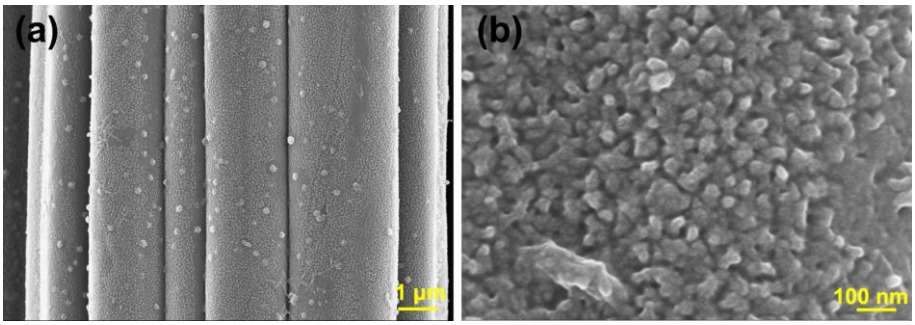

Figure S9 (a) (b) SEM images of AP electrode with 60 min deposition of PANI.

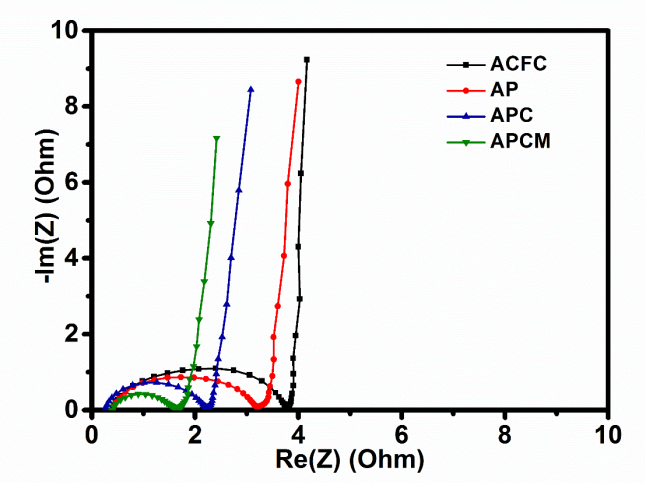

Figure S10. Nyquist plots of different textiles based symmetric aqueous supercapacitors. Nearly vertical lines can be observed at low frequency from all the electrodes, indicating good capacitive performance. In the high-frequency region, the Nyquist plot of APC shows the lowest equivalent series resistance, suggesting small electrode resistance and high charge-transfer rate between the electrolyte and electrodes.

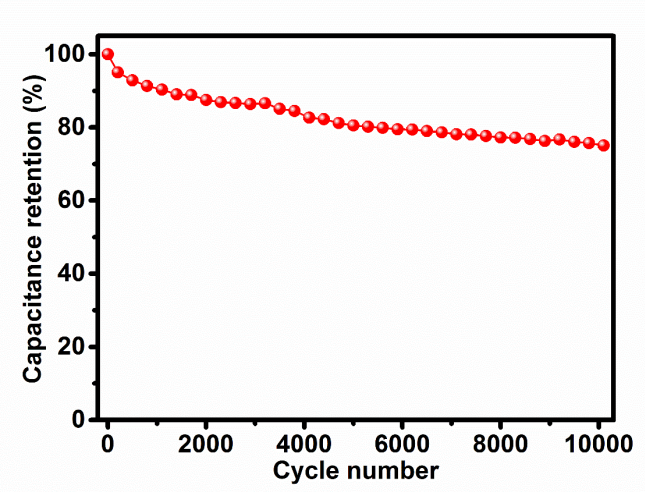

Figure S11. Cycling performance of APCM textile in aqueous symmetric supercapacitor at the current density of 40 mA cm^{-2}.

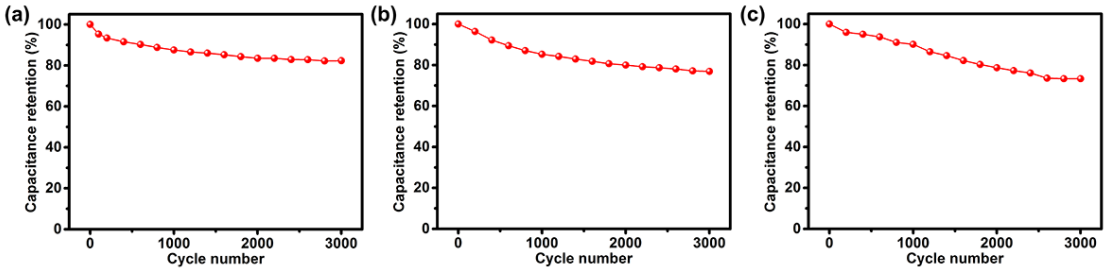

Figure S12. Cycling performance of the flexible solid-state supercapacitors: (a) symmetric textile supercapacitor, (b) asymmetric textile supercapacitor and (c) symmetric fiber-like supercapacitor. Over 3000 charge/discharge cycles (applied current: 4 mA cm^{-2}), about 82 % and 76 % capacitance retention is observed for the symmetric and asymmetric supercapacitors, respectively. And after 3000 charge/discharge cycles (applied current: 0.1 mA cm^{-1}), 73% capacitance retention is observed for the fiber-like supercapacitor.

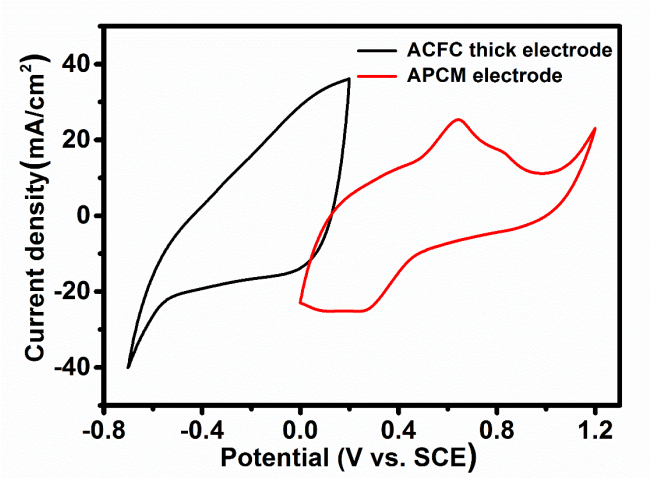

Figure S13. CV curves at 2 mV s^{-1} of the ACFC thick electrode and APCM electrode in 1 M H_2SO_4 solution measured by three-electrode system.

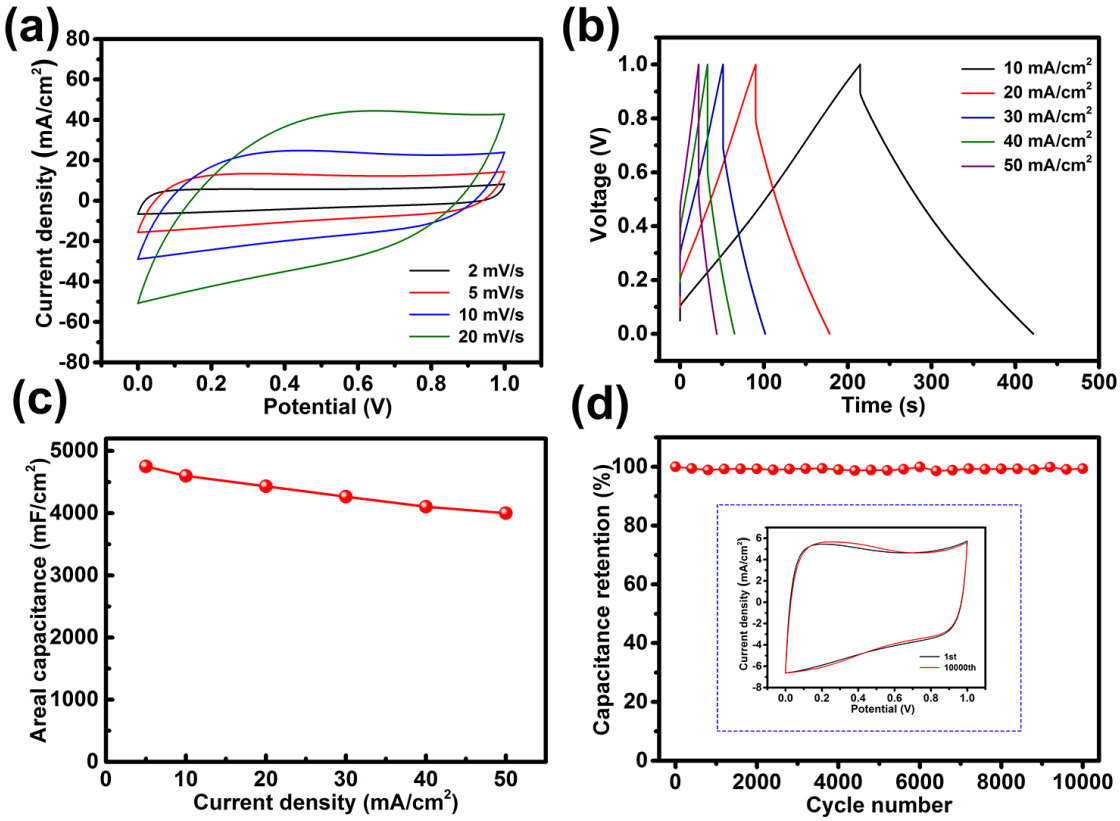

Figure S14. (a) CV curves, (b) GCD curves, (c) capacitance and (d) cycling behavior (applied current of 40 mA cm^{-2}) of ACFC thick electrode in 1 M H_2SO_4 solution.

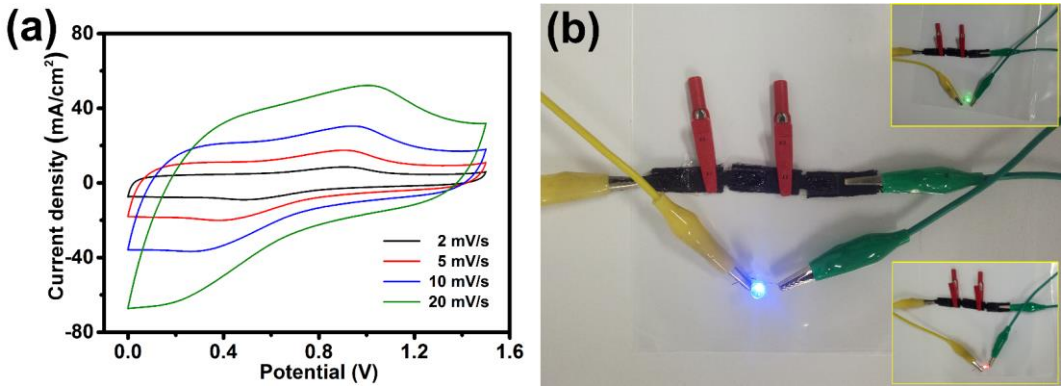

Figure S15. (a) CV curves of the asymmetric aqueous supercapacitor and (b) digital photographs of the flexible solid-state asymmetric textile supercapacitors (3 in series) lighting LEDs.

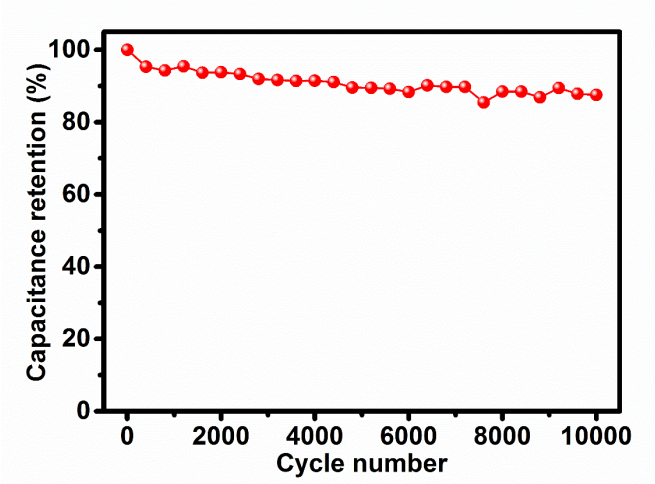

Figure S16. Cycling performance of the APCM fiber-like aqueous symmetric supercapacitor at the current density of 40 mA cm^{-2}.

Table S1. Areal capacitance of various flexible textile electrodes/supercapacitors

No.	Electrode	Areal capacitance	Reference
1	APCM (textile electrode) [a]	4615 mF cm^{-2} at 5 mA cm^{-2}	This work
2	APC (textile electrode) [a]	4165 mF cm^{-2} at 5 mA cm^{-2}	This work
3	AP (textile electrode) [a]	4167 mF cm^{-2} at 5 mA cm^{-2}	This work
4	V_2O_5-PANI/carbon cloth [b]	664.5 mF cm^{-2} at 0.5 mA cm^{-2}	S5
5	PANI/etched carbon fiber cloth [b]	3500 mF cm^{-2} at 1 μA	S6
6	PPy/MnO_2/carbon fiber cloth [b]	228 mF cm^{-2} at 0.14 mA cm^{-2}	S7
7	MnO_2 nano-arrays/carbon fiber cloth [b]	2160 mF cm^{-2} at 5 mA cm^{-2}	S8
8	NiO/MnO_2/carbon fiber cloth [b]	316.37 mF cm^{-2} at 50 mV s^{-1}	S9
9	Fe_2O_3/PPy/carbon fiber cloth [b]	382.4 mF cm^{-2} at 0.5 mA cm^{-2}	S10

10	CoP nanowires/carbon fiber cloth [b]	571.3 mF cm^{-2} at 1 mA cm^{-2}	S3
11	PPy/MnO_2/carbon fiber cloth [b]	2450 mF cm^{-2} at 0.2 mA cm^{-2}	S11
12	FeOOH/carbon fiber cloth [a]	1120 mF cm^{-2} at 1 mA cm^{-2}	S12
13	MnO_2/ZnO/carbon fiber cloth [b]	41.5 mF cm^{-2} at 2 mV s^{-1}	S13
14	$NiMoO_4$/carbon fiber cloth [b]	1270 mF cm^{-2} at 5 mA cm^{-2}	S14
15	Ag/Ni-Co hydroxide/carbon fiber cloth [b]	1133.3 mF cm^{-2} at 1 mA cm^{-2}	S15

[a] : Measured in two-electrode configuration; [b] : Measured in three-electrode configuration.

Table S2. Capacitance of various flexible fiber-like electrodes/supercapacitors

Electrode	Length capacitance	Areal capacitance	Condition	Refer-ence
APCM fiber bundle [a]	116 mF cm^{-1} 90 mF cm^{-1}	756 mF cm^{-2} 588 mF cm^{-2}	2 mV s^{-1} 3 mA cm^{-1}	This work
ERGO/carbon fiber [a]	13.5 μF cm^{-1}	307 mF cm^{-2}	0.05 mA cm^{-1}	S16
Porous core-shell carbon fibers [a]	64.5 mF cm^{-1}	—	10 mV s^{-1}	S17
MnO_2/CNT coiled fiber [a]	2.72 mF cm^{-1}	61.25 mF cm^{-2}	10 mV s^{-1}	S18
Ordered mesoporous car-bon fiber [a]	1.907 mF cm^{-1}	39.67 mF cm^{-2}	0.5 μA	S19
Coaxial all-carbon fiber supercapacitor [a]	6.3 mF cm^{-1}	86.8 mF cm^{-2}	2 mV s^{-1}	S20
MWCNT/MnO_2 compo-site fibers [a]	0.018 mF cm^{-1}	3.53 mF cm^{-2}	0.5 μA	S21

RuO_2•0.4H_2O/carbon fiber [b]	3.2 mF cm^{-1}	146 mF cm^{-2}	1.14 mA cm^{-2}	S22
MnO_2/CNT/nylon fiber supercapacitor [a]	5.4 mF cm^{-1}	40.9 mF cm^{-2}	10 mV s^{-1}	S23

[a] : Measured in two-electrode configuration; [b] : Measured in three-electrode configuration.

References

S1. Dong, L.; Liang, G.; Xu, C.; Liu, W.; Pan, Z.-Z.; Zhou, E.; Kang, F.; Yang, Q.-H., Multi Hierarchical Construction-Induced Superior Capacitive Performances of Flexible Electrodes for Wearable Energy Storage. *Nano Energy* **2017**, 34, 242-248.

S2. Dong, L.; Xu, C.; Li, Y.; Wu, C.; Jiang, B.; Yang, Q.; Zhou, E.; Kang, F.; Yang, Q. H., Simultaneous Production of High-Performance Flexible Textile Electrodes and Fiber Electrodes for Wearable Energy Storage. *Adv. Mater.* **2016**, 28, 1675-1681.

S3. Zheng, Z.; Retana, M.; Hu, X.; Luna, R.; Ikuhara, Y. H.; Zhou, W., Three-Dimensional Cobalt Phosphide Nanowire Arrays as Negative Electrode Material for Flexible Solid-State Asymmetric Supercapacitors. *ACS Appl. Mater. Interfaces* **2017**, 9, 16986-16994.

S4. Zengin, H.; Zhou, W. S.; Jin, J. Y.; Czerw, R.; Smith, D. W.; Echegoyen, L.; Carroll, D. L.; Foulger, S. H.; Ballato, J., Carbon Nanotube Doped Polyaniline. *Adv. Mater.* **2002**, 14, 1480-1483.

S5. Bai, M.-H.; Liu, T.-Y.; Luan, F.; Li, Y.; Liu, X.-X., Electrodeposition of Vanadium Oxide-Polyaniline Composite Nanowire Electrodes for High Energy Density Supercapacitors. *J. Mater. Chem. A* **2014**, 2, 10882-10888.

S6. Cheng, Q.; Tang, J.; Ma, J.; Zhang, H.; Shinya, N.; Qin, L.-C., Polyaniline-Coated Electro-Etched Carbon Fiber Cloth Electrodes for Supercapacitors. *J. Phys. Chem. C* **2011**, 115, 23584-23590.

S7. Fan, X.; Wang, X.; Li, G.; Yu, A.; Chen, Z., High-Performance Flexible Electrode Based on Electrodeposition of Polypyrrole/MnO_2 on Carbon Cloth for Supercapacitors. *J. Power Sources* **2016**, 326, 357-364.

S8. Guo, D.; Yu, X.; Shi, W.; Luo, Y.; Li, Q.; Wang, T., Facile Synthesis of Well-Ordered Manganese Oxide Nanosheet Arrays on Carbon Cloth for High-Performance Supercapacitors. *J. Mater. Chem. A* **2014**, 2, 8833-8838.

S9. Xi, S.; Zhu, Y.; Yang, Y.; Jiang, S.; Tang, Z., Facile Synthesis of Free-Standing NiO/MnO_2 Core-Shell Nanoflakes on Carbon Cloth for Flexible Supercapacitors. *Nanoscale Res. Lett.* **2017**, 12, 171.

S10. Wang, L. B.; Yang, H. L.; Liu, X. X.; Zeng, R.; Li, M.; Huang, Y. H.; Hu, X. L., Constructing Hierarchical Tectorum-Like Alpha-Fe_2O_3/PPy Nanoarrays on Carbon Cloth for Solid-State Asymmetric Supercapacitors. *Angew. Chem. Int. Edit.* **2017**, 56, 1105-1110.

S11. Tao, J.; Liu, N.; Li, L.; Su, J.; Gao, Y., Hierarchical Nanostructures of Polypyrrole@MnO_2 Composite Electrodes for High Performance Solid-State Asymmetric Supercapacitors. *Nanoscale* **2014**, 6, 2922-2928.

S12. Chen, L.-F.; Yu, Z.-Y.; Wang, J.-J.; Li, Q.-X.; Tan, Z.-Q.; Zhu, Y.-W.; Yu, S.-H., Metal-Like Fluorine-Doped β-FeOOH Nanorods Grown on Carbon Cloth for Scalable High-Performance Supercapacitors. *Nano Energy* **2015**, 11, 119-128.

S13. Li, S.; Wen, J.; Mo, X.; Long, H.; Wang, H.; Wang, J.; Fang, G., Three-Dimensional MnO_2 Nanowire/ZnO Nanorod Arrays Hybrid Nanostructure for High-performance and Flexible Supercapacitor Electrode. *J. Power Sources* **2014**, 256, 206-211.

S14. Guo, D.; Luo, Y.; Yu, X.; Li, Q.; Wang, T., High Performance $NiMoO_4$ Nanowires Supported on Carbon Cloth as Advanced Electrodes for Symmetric Supercapacitors. *Nano Energy* **2014**, 8, 174-182.

S15. Sekhar, S. C.; Nagaraju, G.; Yu, J. S., Conductive Silver Nanowires-Fenced Carbon Cloth Fibers-Supported Layered Double Hydroxide Nanosheets As a Flexible and Binder-Free Electrode For High-performance Asymmetric Supercapacitors. *Nano Energy* **2017**, 36, 58-67.

S16. Cao, Y.; Zhu, M.; Li, P.; Zhang, R.; Li, X.; Gong, Q.; Wang, K.; Zhong, M.; Wu, D.; Lin, F.; Zhu, H., Boosting Supercapacitor Performance of Carbon Fibres Using

Electrochemically Reduced Graphene Oxide Additives. *Phys. Chem. Chem. Phys.* **2013**, 15, 19550-19556.

S17. Zhou, W.; Zhou, K.; Liu, X.; Hu, R.; Liu, H.; Chen, S., Flexible Wire-Like All-Carbon Supercapacitors Based on Porous Core–Shell Carbon Fibers. *J. Mater. Chem. A* **2014**, 2, 7250-7255.

S18. Choi, C.; Sim, H. J.; Spinks, G. M.; Lepró, X.; Baughman, R. H.; Kim, S. J., Elastomeric and Dynamic MnO_2/CNT Core-Shell Structure Coiled Yarn Supercapacitor. *Adv. Energy. Mater.* **2016**, 6, 1502119.

S19. Ren, J.; Bai, W.; Guan, G.; Zhang, Y.; Peng, H., Flexible and Weaveable Capacitor Wire Based on A Carbon Nanocomposite Fiber. *Adv. Mater.* **2013**, 25, 5965-5970.

S20. Viet Thong, L.; Kim, H.; Ghosh, A.; Kim, J.; Chang, J.; Quoc An, V.; Duy Tho, P.; Lee, J.-H.; Kim, S.-W.; Lee, Y. H., Coaxial Fiber Supercapacitor Using All-Carbon Material Electrodes. *ACS Nano* **2013**, 7, 5940-5947.

S21. Ren, J.; Li, L.; Chen, C.; Chen, X.; Cai, Z.; Qiu, L.; Wang, Y.; Zhu, X.; Peng, H., Twisting Carbon Nanotube Fibers for Both Wire-Shaped Micro-Supercapacitor and Micro-Battery. *Adv. Mater.* **2013**, 25, 1155-1159.

S22. Wang, J.; Li, X.; Zi, Y.; Wang, S.; Li, Z.; Zheng, L.; Yi, F.; Li, S.; Wang, Z. L., A Flexible Fiber-Based Supercapacitor-Triboelectric-Nanogenerator Power System for Wearable Electronics. *Adv. Mater.* **2015**, 27, 4830-4836.

S23. Choi, C.; Kim, S. H.; Sim, H. J.; Lee, J. A.; Choi, A. Y.; Kim, Y. T.; Lepro, X.; Spinks, G. M.; Baughman, R. H.; Kim, S. J., Stretchable, Weavable Coiled Carbon Nanotube/MnO_2/Polymer Fiber Solid-State Supercapacitors. *Sci. Rep.* **2015**, 5, 9387.